Single-hole injections of liquid hydrocarbon fuels (isooctane and dodecane) under high turbulence have been investigated using direct numerical simulation based on the statistical model considering the droplets' atomization, distribution, and combustion. The study objects are the heat and mass transfer processes during atomization and combustion of liquid fuels injections within the combustion chambers of thermal engines. The temperature and carbon dioxide concentration distributions of the fuel-air mixture, the distributions of the droplets, their velocities, and the Sauter mean radius within the isooctane and dodecane oxidation in the engine's combustion space were obtained. An investigation of the oxidizer's initial temperature influence on the droplets' atomization and combustion processes showed that the optimal temperature for both fuels is 900 K. The obtained modeling results were confirmed in good agreement with theoretical and experimental data.

Thanks to the integrated use of approaches from statistical theory, numerical algorithms and 3D computer modeling techniques, the results obtained are distinguished by high accuracy, efficiency in reducing computational resources, scientific novelty in the type of droplet atomization and suitability for practical application for technological solutions not only for single-hole, but also for multi-hole injections of liquid fuels and studying the jet-to-jet interaction phenomena.

The obtained research results can be applied in miscellaneous internal combustion engines development with different atomization types, which will allow us to contemporaneously settle the concerns of streamlining the combustion process, improving the completeness of fuel combustion and reducing emissions of harmful substances

Keywords: liquid fuel, atomization, combustion, emissions, single-hole injection, thermal engines

UDC 536.2; 502; 519.6
DOI: 10.15587/1729-4061.2024.316100

DETERMINING THE OPTIMAL OXIDATION TEMPERATURE OF NON-ISOTHERMAL LIQUID FUELS INJECTIONS USING MODELING BASED ON STATISTICAL DROPLET DISTRIBUTION

Aliya Askarova
Doctor of Physical and Mathematical Sciences, Professor*
Saltanat Bolegenova
Doctor of Physical and Mathematical Sciences, Professor*
Shynar Ospanova
Corresponding author
PhD, Senior Lecturer*
E-mail: s.osspanova@gmail.com
Symbat Bolegenova
PhD, Associate Professor*
Gulzhakhan Baidullayeva
Candidate of Physical and Mathematical Sciences, Associate Professor
Department of Normal Physiology with a Biophysics Course
Asfendiyarov Kazakh National Medical University
Tole-bi str., 94, Almaty, Republic of Kazakhstan, 050012
Kazyret Berdikhan
Doctoral Student*
Akbota Nussipzhan
Doctoral Student*
*Department of Thermal Physics and Technical Physics
Al-Farabi Kazakh National University
Al-Farabi ave., 71, Almaty, Republic of Kazakhstan, 050040

Received 26.09.2024
Received in revised form 02.12.2024
Accepted 13.12.2024
Published 30.12.2024

Askarova, A., Bolegenova, S., Ospanova, S., Bolegenova, S., Baidullayeva, G., Berdikhan, K., Nussipzhan, A. (2024). Determining the optimal oxidation temperature of non-isothermal liquid fuels injections using modeling based on statistical droplet distribution. Eastern-European Journal of Enterprise Technologies, 6 (8 (132)), 44–55. https://doi.org/10.15587/1729-4061.2024.316100

1. Introduction

At the present energy sector development stage, environmental problems acquire priority significance. It is known that the International Energy Agency has set the task of using up to 80 % renewable energy sources as an energy source by 2050 and halving the emission of carbon dioxide CO_2 into the atmosphere as an indicator of emissions of harmful substances.

Therefore, improving systems and devices for the combustion of various fuel types aims to increase efficiency and reduce the emission of harmful substances into the atmosphere. This is achieved by improving fuel injection systems designed to spray liquid fuels and intensifying heat transfer in power installations [1].

Air pollution is one of the most serious environmental factors affecting the health of every person in many countries with different income levels. The impact of key sources of air pollution can be reduced through policies and investments that promote cleaner modes of transport, improve the energy efficiency of buildings, power generation, and industry, and improve municipal waste management systems. Most sources of air pollution cannot be controlled by individuals, requiring consolidated action by local, national, and regional policymakers in sectors such as energy, transport, waste management, urban planning, and agriculture.

There are many successful policies to reduce air pollution, one of which is the transition to cleaner energy production. In this regard, the adoption of low-emission diesel engines for heavy-duty vehicles, the use of non-polluting vehicles, and eco-friendly fuels, involving sulfur-reduced fuels, is very important. Nowadays in many countries, several methods are used to reduce the amount of harmful vehicle emissions into the atmosphere: continuous improvement of thermal engine models to minimize their fuel consumption, use of sustainable fuels, supply of car exhaust pipes with converters, and creation of green space along roads [2, 3].

The Republic of Kazakhstan ranks 20th among 221 countries in terms of carbon dioxide emissions and 10th in per capita emissions. Greenhouse gas emissions in 2020, according to the latest inventory, amounted to 351 million tons of CO_2 equivalent [4]. Fig. 1 shows annual data on greenhouse emissions in the Republic of Kazakhstan according to statistical data from Our World in Data based on the Global Carbon Project (Fig. 1) [5, 6].

Considering that the Republic of Kazakhstan plans to be in the decarbonization trend, the country plans to achieve carbon neutrality by 2060. The Kazakh government also plans to begin integrating the trading system with state regulation of greenhouse gas emissions and to integrate it with the European system (Fig. 2) [7, 8].

Almaty was among the 100 most environmentally hazardous cities in the world, taking 95th place back in 2019, and since then, environmental activists have not ceased to sound the alarm. The main problems of air pollution in Almaty are vehicle and thermal power plant emissions, poor quality of vehicle fuels, obsolete vehicles, and lack of emission quality control systems [9, 10].

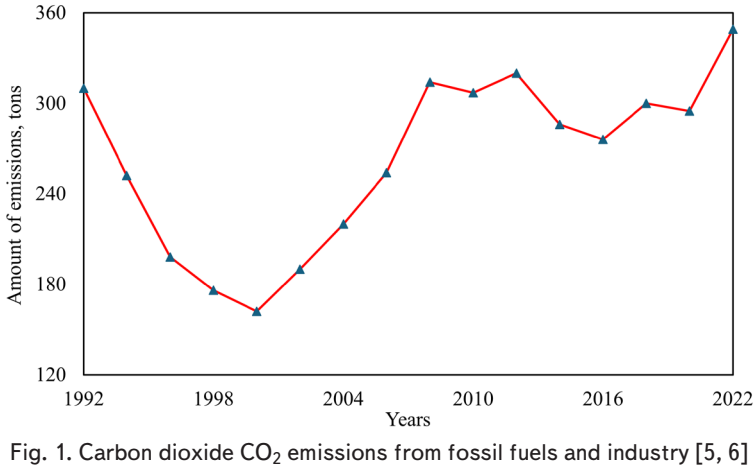

Fig. 1. Carbon dioxide CO_2 emissions from fossil fuels and industry [5, 6]

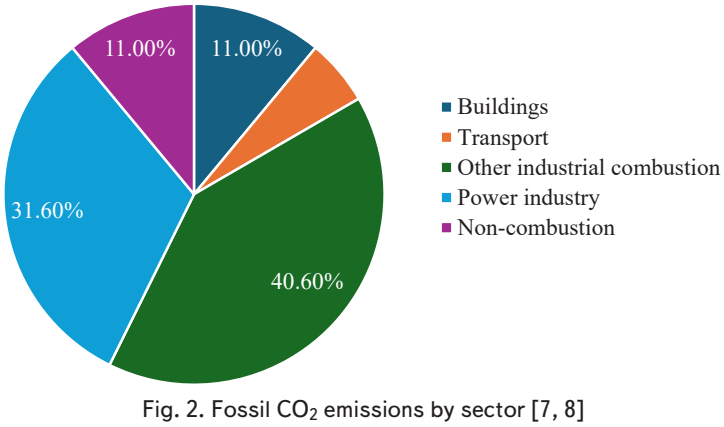

Fig. 2. Fossil CO_2 emissions by sector [7, 8]

Given the fact that all available technologies for fuel preparation and combustion proper have been brought to almost perfection, and the efficiency and environmental friendliness of thermal engines in many cases leave much to be desired, the problem of finding new methods in this area is acute. Modern technologies such as electric vehicles or hybrids certainly help reduce pollution, but they cannot solve the problem of climate warming and deteriorating air quality on their own. The effectiveness of these solutions is limited. Therefore, the optimization of existing fuel injection systems is relevant for the development and improvement of car engines, aimed at increasing their efficiency, reducing pollutant emissions, and improving the overall environmental impact.

Using 3D computer mathematical modeling methods and the latest computing technology allows us to analyze the combustion process under various thermal engine operating conditions and develop new strategies for cleaner combustion under changing factors. Traditional methods of developing and optimizing injection systems require multiple tests, which can be expensive and time-consuming.

The main advantages of using computer modeling methods for efficient and accurate development of various aspects of injection systems, reducing development time, costs and minimizing errors, include optimization of fuel injection parameters, accurate prediction of the combustion process, adaptation to different types of fuel, reduction in the number of physical tests, accelerated optimization of design solutions and increased development accuracy. Thus, modeling makes it possible to check the influence of many parameters, such as pressure, temperature, mass, speed, injection angle, droplet size, and many others, on the combustion processes of different types of fuel to achieve optimal operation of the system in different modes. By optimizing the model during the development process, updated and improved parameters and characteristics of the system are created without the need for physical prototypes development, which are offered to design engineers for their practical implementation.

2. Literature review and problem statement

The paper [11] presents the results of multi-dimensional computer modeling of the atomization and evaporation of liquid fuel injected from a round hole into a compressed gas. Also, phenomenological approaches were used to predict the breakup regimes of droplets of different sizes arising because of the influence of surface tension and aerodynamic forces on the jet at high pressures. When studying various jet breakup regimes depending on the Weber number, its maximum value was 226. At this value, jet breakup usually occurs by the primary atomization mechanism, characteristic of turbulent flows with high inertia. However, due to the limitations of the applied three-dimensional computer model and phenomenological approaches, secondary atomization (at Weber numbers of about 500–1,000) has not been studied, although it is observed when inertial forces prevail over surface tension forces, which leads to smaller fragments.

In significantly high turbulence, where vortices of various scales are present, droplets can

experience even more intense and rapid deformations. In such turbulent multiphase flows, the Weber number for droplets can exceed 1,000 and approach 10,000 due to severe turbulent fluctuations, which was also not considered in [11].

In the work [12], the phenomenon of fragmentation of liquid blobs and filaments under the influence of instabilities of flow surfaces, leading to different droplet distributions within the liquid jet, was studied. The work uses a phenomenological approach, which relies on observations and empirical data rather than detailed modeling of molecular or microscopic phenomena. This implies that the study overlooks factors like molecular forces or the behavior of droplets at the molecular scale, which can greatly influence droplet breakup, particularly at very small sizes. The proposed fragmentation model assumes a fixed droplet shape, which may reduce the accuracy of predictions since in real systems droplets may change their shape depending on the flow. It also overlooks interactions between droplets, such as coalescence and shape deformation, which restricts the model's applicability in complex multi-droplet flows.

Phenomenological models are often inadequate for modeling secondary atomization and droplet fragmentation, as they simplify key processes like heat transfer, chemical reactions, and phase transitions that can have a significant impact on droplet behavior. This leads to reduced accuracy, particularly in complex reacting flows where droplet interactions are considered.

In [13], a model of the primary jet atomization is proposed and applied to high-speed flows to predict its characteristics. The jet breakup characteristics are analyzed by following the wave growth on the surface of each liquid droplet through a one-dimensional Eulerian approach. Similar studies of the atomization and breakup of droplets of fuel jets in reacting media under evaporation conditions based on liquid core fragmentation approaches were carried out experimentally in [14]. Since the Eulerian approach focuses on the average flow characteristics at fixed spatial locations, in [13] and [14] it neglects the finer details of individual particle behavior, as well as their interactions with the turbulent flow. Additionally, the Eulerian approach requires significant computational resources and costs due to the need to track all macroscopic parameters. For complex two-phase flows, where the particle dynamics are significant, the Eulerian approach lacks the necessary accuracy in analyzing the motion of droplets in a jet flow.

Such problems arise due to methodological difficulties, and to solve them it is advisable to use the Lagrangian approach in combination with the statistical distribution of particles, which allows for predicting their behavior, interactions, and influence, as well as distribution in a multiphase flow.

The traditional discrete particle method based on the Euler-Euler (EE) formalism was applied to LES (Large Eddy Simulation) of atomization in the region near the injector by the authors of [15]. Although LES effectively captures large eddies, the influence of small-scale turbulent structures, which are crucial in multiphase flows, is not completely considered in [15]. While LES is a more accurate method, validating the model with real-world conditions is extremely challenging, as relevant experimental data are not always available. This restricts the ability to rigorously evaluate the models and undermines confidence in their outcomes.

Analogous studies were carried out in [16] considering the cavitation effects for a one-dimensional flow of a diesel fuel jet near the nozzle. In [16], a one-dimensional CFD model was used, where all physical processes are described along a single spatial coordinate, without considering variations in other directions. However, in actual multiphase systems, complex chemical reactions and phase transitions, such as evaporation and condensation, frequently occur, which were not considered and resolved in [16], as their simulation demands additional computational resources. Furthermore, due to the simplification of the real flow geometry, local effects like turbulent fluctuations, temperature and concentration gradients, and pressure losses were not included. These factors can significantly affect the accuracy of spray behavior predictions in real systems. Moreover, the limitations of the model prevented the dynamic analysis of complex phenomena such as wave effects, flow pulsations, and stochastic oscillations, which may experience substantial variations in spatial directions and cannot be captured in a one-dimensional statement.

To overcome the previously mentioned issues, arising from mathematical difficulties in solving equations due to limitations in computational grid resolutions, it is recommended to use direct numerical simulation (DNS) for modeling non-isothermal liquid injections, where three-dimensional unsteady turbulent flow equations are solved without the need for special adjustment. Unlike more simplified approaches like RANS or LES, DNS resolves all turbulence scales, providing an accurate description of flow microstructures and allowing the modeling of intricate geometries, where the shape of liquid droplets or bubbles can change depending on the nature of the flow.

In [17], visualization and results of 3D cavitation flow modeling are presented to characterize the cavitation formation inside transparent fuel injector valves used in low-speed two-stroke diesel engines. Resembling studies of visualization of high-speed cavitation structures formed inside diesel engine injectors with changes in liquid spray angles were conducted in [18]. The results of these studies showed a significant increase in the spray angle in the presence of cavitation strings when comparing cylindrical and tapered nozzles. These works are based on numerical simulations, without extensive experimental verification, which reduces confidence in the application of the results to real systems. Steady flow assumptions and simplified nozzle geometry limit the accuracy of the model, and the focus on a limited range of operating conditions reduces the generality of the conclusions for all operating modes of direct injection (DI) engines.

To solve the problems highlighted in these works, it is necessary to perform experimental validation of numerical models, consider the non-isothermal nature of injection and reacting flows, account for phase and droplet interactions, use more advanced models of injector nozzle geometry, and expand the range of operating conditions. This will enhance the accuracy of predictions and the applicability of conclusions across various engine operating modes.

To study non-isothermal injections of various liquid fuels, it is recommended to use direct numerical simulation and statistical approaches, which better capture particle distribution, primary and secondary atomization, and the energy spectra of turbulent vortex structures. This approach is ideal for optimizing combustion processes and improving engine efficiency, addressing both detailed dynamics and macroscopic flow behavior.

3. The aim and objectives of the study

The aim of the study is to determine the oxidation temperature influence on heat and mass transfer processes during atomization and combustion of single-hole non-isothermal injections of two types of liquid fuels (isooctane and dodecane)

by conducting computational experiments using direct numerical simulation based on statistical droplet distribution. These studies will contribute to the optimization of liquid fuel combustion processes in combustion chambers of thermal engines to improve process parameters, increase fuel combustion efficiency, and reduce harmful emissions.

To achieve this aim, the following objectives are accomplished:

– to construct a statistical model to describe the atomization, distribution, and combustion of droplets under high turbulence;

– to determine the optimal value of the oxidizer's initial temperature based on its influence on the maximum combustion temperature and the carbon dioxide concentration distribution;

– to apply a statistical model for 3D visualization of temperature, concentration, and aerodynamic characteristics of the reacting flow;

– to validate the obtained results by comparing them with theoretical and experimental data.

4. Materials and methods

4. 1. Object and hypothesis of the study

The object of the study is the heat and mass transfer processes during the atomization and combustion of liquid fuels (isooctane and dodecane) injections in the combustion chambers of direct injection (DI) engines.

The study's main hypothesis is that the oxidizer's initial temperature significantly affects the heat and mass transfer processes during the combustion of non-isothermal injections of liquid hydrocarbon fuels (gasoline and diesel) in the combustion chambers of thermal engines. At the same time, there is an optimal oxidation temperature at which the efficiency of fuel combustion increases, the quality of droplet atomization improves, and emissions of harmful substances are minimized. Determining this temperature using direct numerical simulation and a statistical approach allows us to accurately describe the droplet atomization, distribution, and combustion processes under high turbulence. It offers optimal conditions for organizing the rational combustion of fuels in injection systems.

Assumptions made in the study are:

– the combustion process of liquid hydrocarbon fuels follows a non-isothermal injection model, where temperature variations are considered within the combustion chamber;

– the oxidation temperature significantly impacts the heat and mass transfer processes during droplets' atomization, distribution, and combustion;

– the droplets are modeled using a statistical distribution approach, and their behavior under high turbulence is accurately represented in the simulation;

– the combustion chamber's environment is assumed to be a controlled system with a direct injection mechanism for fuel supply;

– the chamber wall temperature is assumed to be constant;

– the study assumes a constant high turbulence level, which is typical in the combustion chambers of DI engines;

– the atomization, distribution, and combustion of droplets are analyzed while accounting for potential interactions between droplets, including collision and coalescence effects;

– the optimal oxidation temperature is assumed to maximize fuel combustion efficiency, improve droplet atomization quality, and minimize harmful emissions.

Simplifications adopted in the study are:

– the fuel compositions were assumed to be nearly ideal, disregarding impurities using averaged properties;

– before injection, the fuel droplets were assumed to have a uniform size;

– evaporation and droplet dynamics, including their distribution and collisions, were modeled separately from combustion kinetics;

– to simplify the chemical kinetics of oxidation, a one-step combustion model was used;

– the study focused on a single-hole fuel injection system, excluding multi-hole injection effects and jet-to-jet interactions, simplifying the analysis;

– the droplet distribution and behavior were assumed to follow statistical distributions, avoiding the need for complex individual droplet simulations.

4. 2. Physical and mathematical models of the problem

Solving the problem of atomization, dispersion, and evaporation of liquid droplets and their interaction with the gas phase is an extremely complex problem. One must consider the distribution of droplet sizes, velocities, and temperature to calculate the mass, angular momentum, and heat transfer between an evaporating droplet and a gas. The mathematical problem of atomization and combustion of non-isothermal liquid injections is based on the conservation equations of mass, momentum, internal energy, and concentration. The mathematical model of the problem includes the following system of equations.

The equation of conservation of mass is written as follows [19]:

$$\frac{\partial \rho}{\partial t} + div(\rho u) = S_{mass}, \quad (1)$$

where u is the fluid velocity. Since a gas-liquid mixture is considered in this way, the source term S_{mass} represents a local change in the density of the gas due to evaporation or condensation.

The momentum conservation equation for the gas is as follows [19, 20]:

$$\rho \frac{\partial u}{\partial t} + \rho(gradu)u = div\xi + \rho g + S_{mom}. \quad (2)$$

For a two-phase flow, the source term on the right side of the equation S_{mom} represents the local rate of momentum change in the gas phase due to the motion of drops.

The internal energy conservation equation is as follows [19, 20]:

$$\rho \frac{\partial E}{\partial t} = \tau : D - \rho divu - divq + S_{energy}, \quad (3)$$

where the source term S_{energy} denotes the contribution to the change in internal energy due to the presence of the atomized liquid phase.

The concentration conservation equation for the component m is [21]:

$$\frac{\partial(\rho c_m)}{\partial t} = -\frac{\partial(\rho c_m u_i)}{\partial x_i} + \frac{\partial}{\partial x_i}\left(\rho D_{c_m} \frac{\partial c_m}{\partial x_i}\right) + S_{mass}, \quad (4)$$

where ρ is the total mass density.

4. 3. Geometric model of the problem

Multi-hole injectors provide a more efficient way to atomize the fuel, helping to reduce fuel injection time and penetration length and improve air-fuel mixture quality with sufficient vapor uniformity, which is the best process condition [22]. However, the presence of many holes is difficult due to closely spaced spray jets, the nature of which is generally very unpredictable at high loads. This distinctive feature of closely spaced flares, leading to their interaction, called the jet-on-jet phenomenon, has not yet been thoroughly studied. In addition, at high temperatures, the jet-to-jet interaction is difficult to control and can cause the entire jet to break up. For a more detailed understanding of the nature and structure of atomization of liquid fuels, it is more expedient to begin with studying single-hole continuous fuel injection, which can be easily manipulated using computer technology.

Modern combustion engines rely on advanced fuel injectors to deliver fuel to the engine in the most efficient way. There are different kinds of fuel injection systems, depending on the engine type. The most used thermal engines are spark ignition (SI) [23], port injection (PFI) [24], and direct injection (DI) engines. In gasoline direct injection (GDI) engines, fuel is injected directly into the cylinder during the intake or compression stroke of the thermal engine according to engine load conditions. Under high operating load conditions, fuel is injected during the intake stroke and the engine operates as a uniformly charged stoichiometric spark ignition engine [25]. By minimizing pump losses, heat loss, and high compression ratios, DI engines are up to 15 % more fuel-efficient.

The prototype of the DI engine was used in the work, in which fuel is directly sprayed through one of the single nozzle holes under 200 bar (Fig. 3) [26].

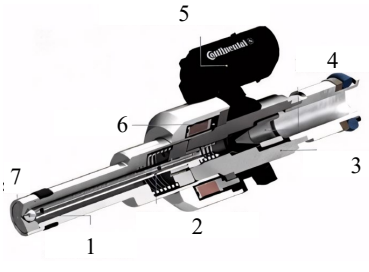

Fig. 3. Schematic view of a direct injection (DI) engine: 1 — injector tip; 2 — piston; 3 — injector shell; 4 — fuel delivery system; 5 — wire connector; 6 — power transmission system; 7 — atomizer

Direct injection diesel engines operate at significantly higher pressures, on average 10 times higher than the values typical for spark ignition engines.

Liquid fuels sprayed into the engine's combustion chamber create ring-like spray patterns. Commonly, liquid jets are formed near the injector nozzle, which, moving further downstream, breakup into droplets under the influence of air, leading to increased instability on the surface of the liquid.

Droplet fragmentation continues further along the flow, which contributes to their subsequent evaporation. Moreover, compared to intake port injection, some direct injection strategies help to achieve higher peak cylinder pressure. High temperatures in thermal engine chambers promote NOx formation, but in-cylinder fuel distribution can effectively reduce CO, CO_2, and soot emissions.

A cylindrical combustion chamber model was used, built by analogy with the spray mechanism and geometric characteristics of a direct injection engine. The height (Z or H) of which is 15 cm, and the diameter is 4 cm. The general view of the combustion chamber is shown in Fig. 4. Liquid fuel is supplied directly into the combustion chamber through the injector nozzle located in the lower part.

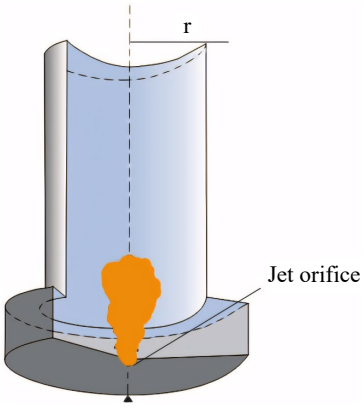

Fig. 4. General view of the combustion chamber

Isooctane C_8H_{18} and dodecane $C_{12}H_{26}$ are used, which are the main components of gasoline and diesel fuel. Isooctane is found in small amounts in straight-run gasoline and is used as an additive in the production of gasoline to improve its anti-knock properties. Dodecane is also used for analytical purposes in the study of the composition of oil fractions.

5. Results of the study on heat and mass transfer processes during atomization and combustion of single-hole injections influenced by oxidation temperature

5. 1. Statistical model construction

A statistical model of liquid fuel droplets' atomization, distribution, and combustion under high turbulence was constructed.

The probability density function of droplet size distribution with an increasing number of their breakup and collisions between them has the following form [13, 20]:

$$f(r)=\frac{1}{r\sqrt{2\pi\sigma^2}}e^{-\frac{\left(\ln r-\langle\ln r\rangle\right)^2}{2\sigma^2}}, \quad (5)$$

where r is the radius of the droplets, σ is the standard deviation describing the degree of droplet size dispersion relative to their average logarithmic value. This distribution is applied when droplet sizes span a broad range and cannot take on negative values.

When a particle moves in a turbulent gas stream with large-scale structures much larger than the diameter of the particle, the relative velocity between the particle and the gas stream is determined as follows [20]:

$$\frac{dv_p}{dt}=\frac{\left(v_g-v_p\right)\left|v_g-v_p\right|}{\tau_{St}}. \quad (6)$$

When calculating many turbulent flows coupled with liquid atomization, it is also necessary to consider drop fluctuations, distortions, and breaks, therefore, for the calculation of internal combustion engines, it is very important to consider the droplets' collisions with each other and their combination

into larger drops. When a liquid is sprayed and filaments are crushed into drops, the main factors determining the disintegration of drops are the densities of the liquid and gas phases, the relative velocity between the liquid and the gas phase, and the viscosity and surface tension of the liquid.

The Weber number, which is defined as the ratio of the degree of inertness of the liquid to the surface tension, becomes the decisive dimensionless number in the breakup of drops [11, 27]:

$$We_p = \frac{\rho_g \left| u_g - u_p \right|^2 r_p}{\sigma_p}, \quad (7)$$

where ρ is the fuel droplets' density, and σ_p is the fuel droplets' interfacial tension coefficient.

At high turbulence, the instantaneous value of the Kolmogorov length scale is much smaller than the particle size, which implies that the full spectrum of turbulent kinetic energy contributes to the expansion and breakup of droplets. The critical droplet radius is determined from the balance of destructive hydrodynamic and capillary forces:

$$r_{cr} = \left(\frac{9}{2} \frac{We_{cr} \sigma \nu_{lam}}{\varepsilon \rho} \right)^{1/3}, \quad (8)$$

where ν_{lam} is the kinematic viscosity coefficient, and ε is the viscous dissipation rate. The turbulent viscosity is consequently determined by the energy spectrum of vortices with scales smaller than the particle's diameter. Fig. 5 provides an illustration of this phenomenon.

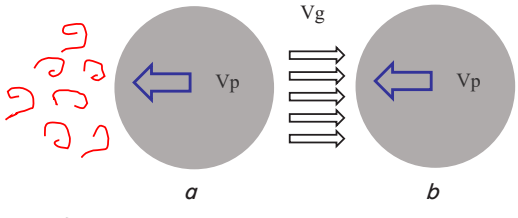

Fig. 5. Comparison of droplet sizes with the scales of turbulent structures: *a* — motion of a droplet whose size surpasses the vortex structures; *b* — motion of a droplet whose dimensions are within the scale of turbulent structures

The finite element method (FEM) is used for numerical simulation of complex two-phase flow through discretization of the domain into a finite number of elements, which allows for complex geometries and conditions at phase boundaries. Along with the use of direct numerical simulation, FEM makes it possible to describe the dynamics of a two-phase flow, including the mechanisms of droplet collision and coalescence, heat exchange between phases through evaporation, and phase transitions [28, 29].

5. 2. Oxidizer's optimal initial temperature determination

The influence of the initial temperature of the oxidizer in the combustion chamber at values from 700 K to 1,500 K on the processes of atomization, distribution, and combustion of two types of liquid fuels (isooctane and dodecane) droplets under high turbulence was investigated. The optimal values of pressure and mass were extracted from the authors' previous works [30]: for isooctane, the pressure and mass values were 100 bar and 6 mg, respectively, and for dodecane, they were 80 bar and 7 mg. Accordingly, all calculations were carried out with these optimal process parameters.

The dependence of the maximum combustion temperature (Fig. 6) and the carbon dioxide concentration distribution (Fig. 7) on the oxidizer initial temperature in the combustion chamber were obtained.

When the oxidizer temperature *T* in the combustion chamber exceeds 800 K, the fuel combustion process becomes more intense, and a high amount of heat is produced, which leads to heating of the combustion chamber to almost 3000 K (Fig. 6).

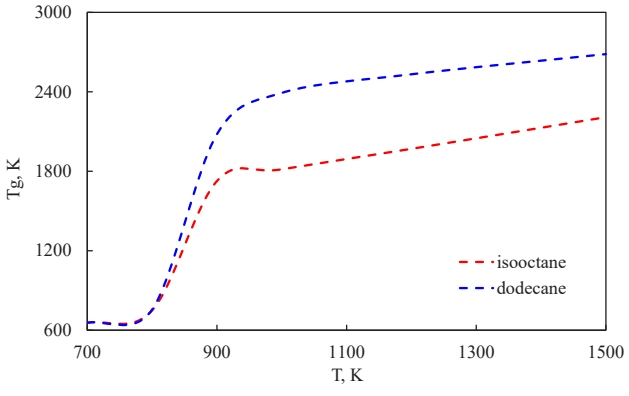

Fig. 6. Dependence of the maximum combustion temperature T_g on the oxidizer initial temperature *T* in the model chamber while isooctane and dodecane burning

Fig. 7 shows the distribution of the maximum concentration of carbon dioxide CO_2 for two fuels (isooctane C_8H_{18} and dodecane $C_{12}H_{26}$) depending on the oxidizer initial temperature in the model chamber. We see that as dodecane burns, the concentration of carbon dioxide generated surpasses that of isooctane.

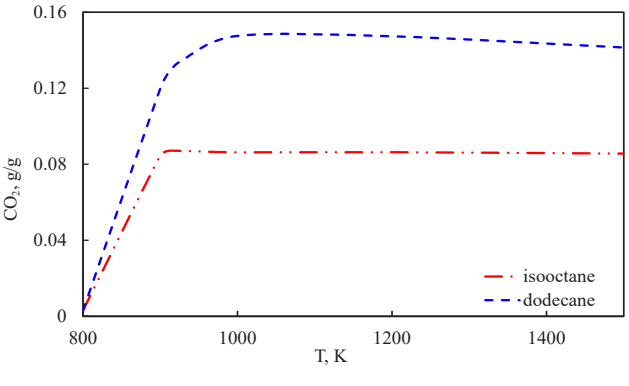

Fig. 7. Effect of the oxidizer initial temperature *T* on the carbon dioxide CO_2 concentration distribution while isooctane and dodecane burning

According to Fig. 6, 7, it is clear that for isooctane and dodecane, the most effective initial temperature of the oxidizer in the combustion chamber is 900 K. Under these temperature conditions, the fuel quickly interacts with the oxidizer, which leads to heating of the chamber to high temperatures, while the concentration of carbon dioxide remains within acceptable limits.

5. 3. Application of a statistical model for 3D visualization of reacting flow characteristics

Fig. 8–10 show the results of 3D visualization of temperature fields, distribution of carbon dioxide concentration, and dispersion of isooctane and dodecane droplets by size along

the combustion chamber height at a time of t=3 ms. These three-dimensional graphs were obtained at the optimal initial oxidizer temperature of 900 K, established in section 5. 3.

Fig. 8 shows a 3D visualization of temperature fields during the combustion of isooctane and dodecane at a time of t=3 ms at the optimal oxidizer temperature (900 K).

When the mixture of fuel vapors with an oxidizer is ignited, the fuel starts to burn quickly, because of which most of the width of the chamber is covered by a flame. A comparison of these graphs shows that during isooctane's combustion, the maximum temperature T_g reaches 1,726 K (Fig. 8, *a*), and when dodecane ignites, the highest temperature T_g attains 2,080 K (Fig. 8, *b*). This means that the dodecane flame reaches high-temperature values, which is confirmed by the results presented in Fig. 6.

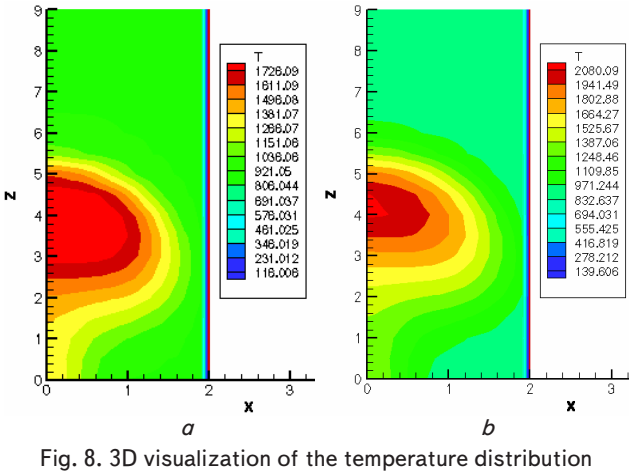

Fig. 8. 3D visualization of the temperature distribution throughout the chamber volume when isooctane C_8H_{18} and dodecane $C_{12}H_{26}$ burning at the moment of time t=3 ms: *a* – isooctane, *b* – dodecane; *Z* (cm) – chamber's height projection; *X* (cm) – chamber's longitudinal projection

Fig. 9 shows a three-dimensional visualization of the distribution of carbon dioxide CO_2 along the height of the combustion chamber at a time of t=3 ms during the combustion of isooctane and dodecane at the optimal oxidizer temperature (900 K). An analysis of these figures shows that the maximum amount of carbon dioxide for isooctane is formed on the combustion chamber axis, which is 0.085 g/g (Fig. 9, *a*). When dodecane burns at the combustion chamber's central axis, the concentration of generated carbon dioxide reaches 0.119 g/g (Fig. 9, *b*). At the combustion chamber outlet, the carbon dioxide concentration decreases and takes on minimal values for both fuels. At an optimal temperature of 900 K, the carbon dioxide concentration for isooctane is 0.006 g/g, and for dodecane is 0.008 g/g.

Fig. 10 shows the distribution of two fuels (isooctane and dodecane) droplets in the combustion chamber space at the optimal oxidizer temperature (900 K). The temperature distribution of the fuel droplets showed that the temperature in the chamber at the moment of time t=3 ms during the combustion of isooctane reaches 547 K, and for dodecane, it reaches 629 K at 3 ms (Fig. 10). The zone of intensive evaporation for isooctane is in the region of 0.5–1 cm along the height of the combustion chamber, and 0.2 cm in width. For dodecane, this region is located at 0.5–1.4 cm and 0.2 cm, respectively. As the temperature of the oxidizer increases, the droplet temperature increases for both fuels.

Fig. 11, 12 show 3D visualization of the distributions of the velocities and droplets' Sauter mean radius during the combustion of isooctane and dodecane at a time of t=3 ms at the optimal initial oxidizer temperature (900 K).

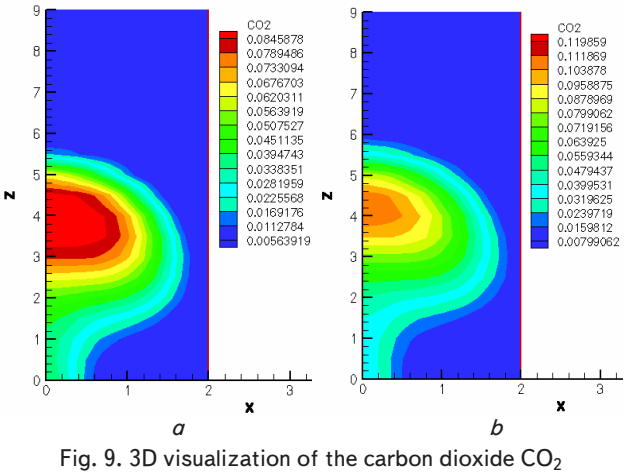

Fig. 9. 3D visualization of the carbon dioxide CO_2 concentrations distributions when isooctane C_8H_{18} and dodecane $C_{12}H_{26}$ burning at the moment of time t=3 ms: *a* – isooctane, *b* – dodecane; *Z* (cm) – chamber's height projection; *X* (cm) – chamber's longitudinal projection

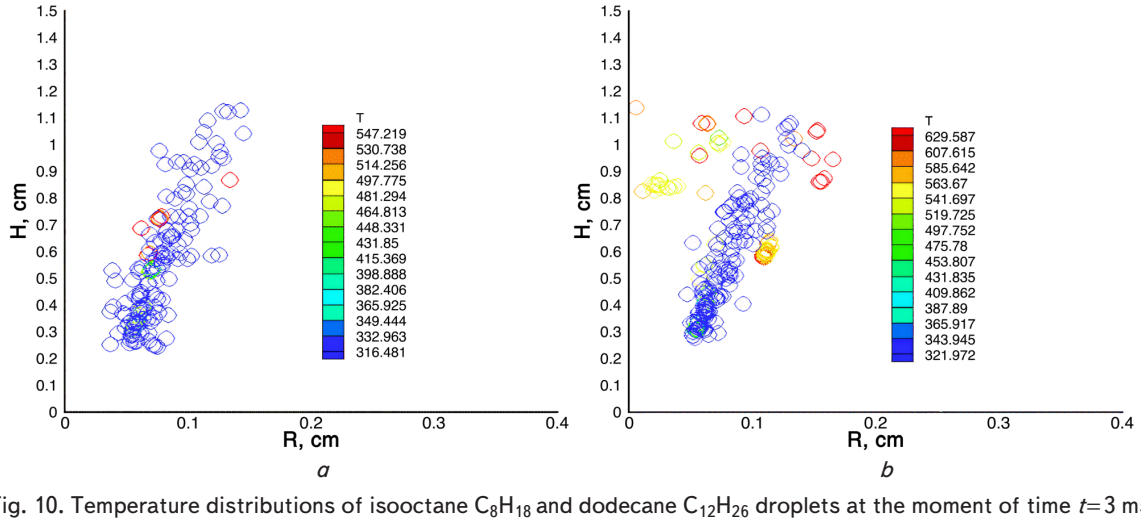

Fig. 10. Temperature distributions of isooctane C_8H_{18} and dodecane $C_{12}H_{26}$ droplets at the moment of time t=3 ms: *a* – isooctane, *b* – dodecane; *H* – chamber's height projection; *R* – chamber's longitudinal projection

Fig. 11 shows the longitudinal component of the isooctane and dodecane droplets' velocity (w) allocation at the moment of time t=3 ms. On the axis of the combustion chamber, the droplets' velocity reaches a maximum value of 550 cm/s, and the rest of the droplets' velocity of both fuels is 50 cm/s.

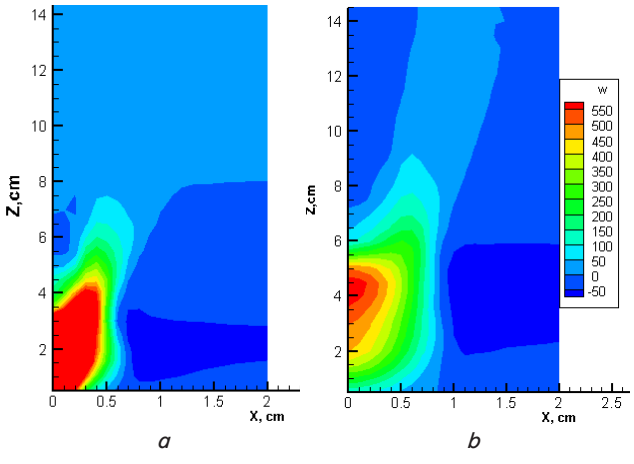

Fig. 11. Isooctane and dodecane droplets velocity (w) distribution along the chamber at the moment of time t=3 ms: a – isooctane, b – dodecane; Z – chamber's height projection; X – chamber's longitudinal projection

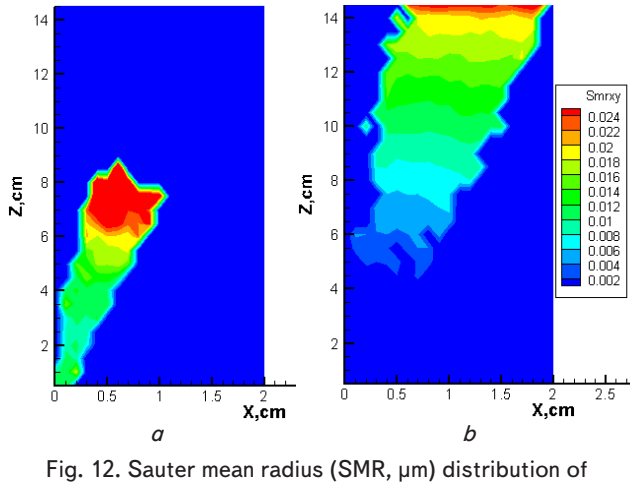

Fig. 12. Sauter mean radius (SMR, μm) distribution of isooctane and dodecane droplets in the chamber space at the moment of time t=3 ms: a – isooctane; b – dodecane; Z – chamber's height projection; X – chamber's longitudinal projection

Fig. 12 shows the distribution of isooctane and dodecane droplets' Sauter mean radius (SMR) throughout the space of the combustion chamber at the moment of time t=3 ms. This visualization illustrates the size distribution of fuel particles throughout the combustion chamber. As can be seen from Fig. 12, large droplets are focused in the chamber's lower area. Then the combustion chamber warms up to high temperatures, and then over time, under the influence of small-scale vortex structures, the particles move to the exit of the combustion chamber.

5. 4. Validation of the obtained results

Fig. 13 compares the results of numerical simulation and experimental data on the size distribution of isooctane droplets after injection starts. The distribution of the mean droplet size D at different distances L from the jet axis is measured at different time moments from 1.6 ms to 2 ms. At the start of the injection, the initial size of the droplets was 10 μm, as they moved downstream of the jet, they acquired values of 7.43 μm in numerical simulation, and in the experimental study, it was 7.55 μm [31]. 40 mm downstream of the injector nozzle, the average droplet size in the experiment decreased to 5.89 μm, while in numerical simulation, it reached 6.55 μm.

The numerical simulation results were compared with experimental data [31] and known theoretical [32] probability density functions for the size distribution of droplets (Fig. 14).

Fig. 15 shows the measurement results of the liquid fuel injection penetration length into the combustion chamber at different time moments.

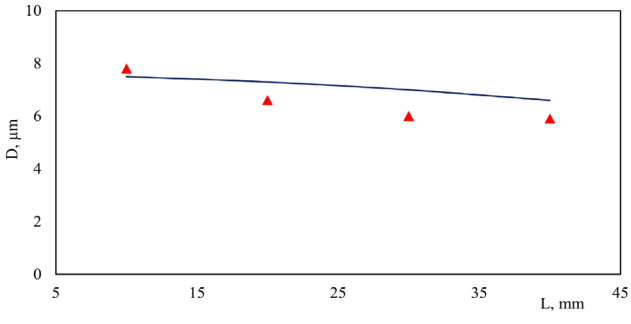

Fig. 13. Distribution of the mean droplet diameter (D) at different distances (L) from the injector nozzle for single-hole injection: solid line – numerical data, Δ – experiment [31]

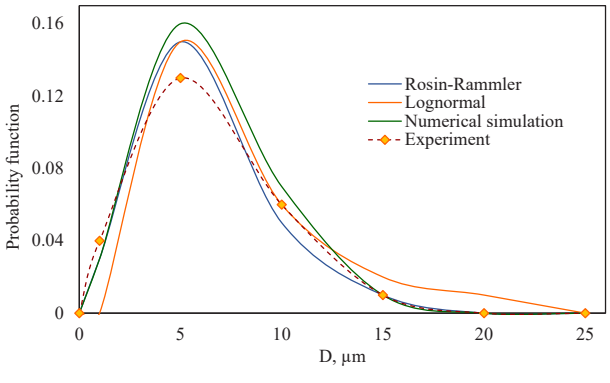

Fig. 14. Comparison of the size (D) distribution probability of isooctane droplets with theoretical [32] and experimental [31] data

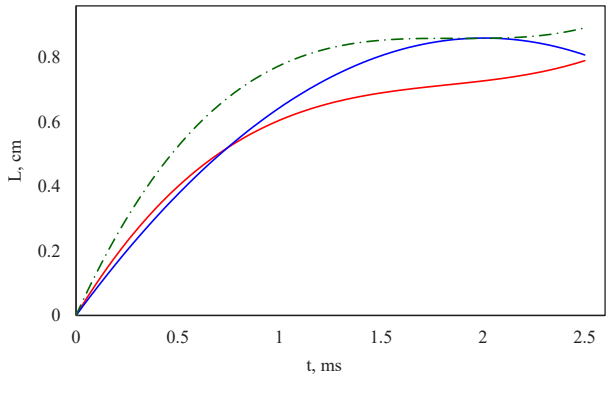

Fig. 15. Liquid fuel injections penetration length (L) into the combustion chamber at different time moments (t): green line – diesel fuel, experiment [33], blue line – dodecane, red line – isooctane

The simulation results for isooctane, dodecane, and experimental data [33] for diesel fuel were compared (Fig. 15). In [33], tetradecane was used in the experiment, which, along with dodecane, is used in the composition of diesel fuel. The initial difference in the results can be attributed to the fact that isooctane is primarily found in gasoline, which has a much lower surface tension compared to diesel fuel.

All numerical calculations were performed considering the electrical and hydraulic time delays, as detailed in [34, 35]. We factored in this delay in the numerical simulations to ensure the fuel injection start time aligned with the experiment.

6. Discussion of research results on heat and mass transfer processes during atomization and combustion of single-hole injections influenced by oxidation temperature

The developed statistical model (5)–(8) enabled the inclusion of not only droplet breakup, collision, and coalescence mechanisms but also the influence of turbulent structures of various scales on their dispersion and size distribution throughout the entire reacting volume, something that was previously unfeasible within the scope of phenomenological approaches to predicting spray behavior [11, 36].

Analyzing the two-dimensional graphs of the dependences of the maximum combustion temperature of isooctane and dodecane in Fig. 6, it can be noted that the oxidizer's initial temperature has the main influence on the combustion of dodecane. Increasing it from 900 K to 1,500 K leads to an increase in the greatest temperature T_g from 2080.09 K to 2684.69 K. For isooctane the highest temperature T_g rises from 1726.09 K to 2208.53 K.

Under high turbulence conditions, with the combined use of numerical simulation and a statistical approach, it became possible to develop a highly efficient model for calculating single-hole injection, achieving significantly high-temperature values (up to 3,000 K). This contrasts with standard conditions, where analytical calculations [37] typically show that the flame temperature during the combustion of gasoline and diesel fuel usually ranges between 1,500–1,800 K.

Combustion of hydrocarbon fuels does not occur at temperatures below 800 K (Fig. 6) [33]. Raising the oxidizer's temperature speeds up the combustion, leading to a more thorough carbon oxidation. At low temperatures, combustion may be inefficient, resulting in the production of not only CO_2 but also other byproducts like carbon monoxide (CO), soot particles, and nitrogen oxides. Since the complex model enabled the attainment of high combustion temperatures, it was observed that at oxidizer temperatures above 900 K, the combustion of liquid fuels becomes more efficient, facilitating faster and more complete combustion of hydrocarbons (Fig. 7). This enhances process efficiency and reduces the harmful emissions formation.

The combined use of a statistical model for atomization and droplet distribution with numerical simulation allowed for a more precise determination of 3D temperature contours, flame height and core (Fig. 8), carbon dioxide concentration profiles (Fig. 9), and droplet distribution by temperature (Fig. 10), velocity (Fig. 11), and size (Fig. 12) under the influence of various vortex structures. This contributed to the optimal process parameter (oxidizer temperature) determination and a deeper understanding of the properties of single-hole injection and two-phase flows.

The validation of the accuracy and convergence of the constructed complex model demonstrated that the numerical simulation for isooctane aligns well with the experimental distribution of droplets by size (Fig. 13) and the two most widely used standard particle distribution functions in the engineering literature: the log-normal distribution and the Rosin-Rammler distribution [32] and experimental data [31] (Fig. 14). It is also important to highlight that the equations (5)–(8) that have been chosen for constructing the statistical model are the most appropriate for depicting droplet behavior in single-hole injection.

Validation of the obtained results of numerical modeling will help to avoid the use of unreliable data, which can lead to significant errors in thermal engine design.

A comparative analysis of the numerical simulation of the injection penetration lengths of various fuels with the experimental data (Fig. 15) demonstrated strong agreement, as the modeling considers that the surface tension of tetradecane is significantly higher than that of dodecane and isooctane, which influences the droplet evaporation rate. This characteristic of diesel fuel is often overlooked in many studies, leading to modeling results with significant errors that reduce their practical applicability. This is the primary benefit of this study.

The presented studies' results have practical applications for implementing single-hole non-isothermal injections for various types of liquid hydrocarbon fuels (gasoline, diesel) in internal combustion engines with direct injection. Furthermore, the optimal process parameters identified during the study can also be applied to multi-hole DI injectors, optimizing the combustion process of fuels and reducing harmful gas (CO_2) emissions.

On the other hand, the relevance of the obtained results to multi-hole injections may be restricted, as increasing the number of injection jets leads to challenges in modeling phenomena such as jet-to-jet interaction.

Since the results obtained pertain to gasoline and diesel internal combustion engines, their application is unfeasible for aircraft and rocket engines, as well as other types of injectors, where air-blast atomization spray mechanisms and non-direct injection types are dominant.

The constructed complex model, including a statistical approach for describing the atomization and distribution of particles of liquid hydrocarbon fuels, can be improved and further developed for application to the study and improvement of the combustion of biofuels (biodiesel) in the combustion chambers of thermal engines without requiring substantial modifications to their design.

7. Conclusions

1. A statistical model for describing the atomization, distribution, and combustion of droplets under high turbulence was constructed and applied for direct numerical simulation of non-isothermal single-hole injection of two types of liquid fuels (isooctane and dodecane) in the combustion chamber of the thermal engine. The application of the statistical model enabled the consideration of mechanisms such as droplet breakup, collision, and coalescence, as well as the impact of various turbulent structure scales on droplet atomization and distribution by temperature, size, and velocity throughout the entire combustion chamber volume.

2. The optimal initial temperature of the oxidizer is determined based on its influence on the distribution of the

maximum combustion temperature and the concentration of carbon dioxide in the combustion chamber. It has been determined that raising the oxidizer temperature above 900 K results in a rise in the maximum combustion temperature of fuels (exceeding 3,000 K), their rapid and complete combustion, and a decrease in the reduction of harmful gas emissions.

3. The combined application of a statistical model of atomization, distribution, and combustion of fuel droplets along with direct numerical simulation made it possible to obtain 3D visualizations of the reacting flow throughout the entire combustion chamber volume:

– three-dimensional temperature contours for isooctane reached a maximum temperature of 1,726 K, and for dodecane was 2,080 K, which significantly exceeds the values (1,500 K) obtained using standard calculation methods;

– the flame height of isooctane varied from 3 to 5 cm, and that of dodecane from 3.6 to 4.9 cm. The flame core of isooctane was more defined, extending up to 1.6 cm in width, while for dodecane it remained narrow, not exceeding 0.8 cm;

– the carbon dioxide concentration profiles for both fuels showed maximum values at the combustion chamber axis (up to 0.1 g/g) and minimum values at the outlet (no more than 0.01 g/g);

– the droplet distributions by temperature, velocity, and size showed the following maximum values: the specific temperature of isooctane droplets was 547 K, while for dodecane it was 629 K; the droplet velocity of both fuels was 550 cm/s; the Sauter mean radius of the large droplets in the lower part of the chamber was 24 μm, while the other smaller droplets ranged from 2 to 4 μm in size.

This two-phase flow visualization enabled the determination of an optimal oxidizer temperature and a comprehensive analysis of the characteristics of non-isothermal hydrocarbon fuel injections.

4. Validation of the obtained modeling results showed the adequacy, reliability, and applicability of the constructed complex model, including a statistical approach, in comparison with theoretical and experimental data on the distribution of droplets by size and the penetration length of injections of various types of fuels. In the simulation, the smallest droplets with sizes from 7.43 to 6.55 μm were calculated, while in the experiment from 7.55 to 5.89 μm. When compared with theoretical distribution functions (Rosin-Rammler and lognormal), the function maximum (f_{max}=0.15–1.16) for all distributions, including modeling, is achieved at a droplet size of 5 μm, which confirms good convergence and adequacy of the model. Injection penetration length measurements showed good agreement between dodecane and experimental diesel fuel data, where the penetration length was 0.74–0.88 cm at a time of 1.5–2.5 ms, while for isooctane this value varied from 0.62 to 0.82 cm.

Conflict of interest

The authors declare that they have no conflict of interest in relation to this research, whether financial, personal, authorship, or otherwise, that could affect the research and its results presented in this paper.

Financing

This work was supported by the Science Committee of the Ministry of Science and Higher Education of the Republic of Kazakhstan [grant number AP19679741].

Data availability

The manuscript has no associated data.

Use of artificial intelligence

The authors confirm that they did not use artificial intelligence technologies when creating the current work.

References

1. Messerle, V. E., Askarova, A. S., Bolegenova, S. A., Yu Maximov, V., Nugymanova, A. O. (2019). 3D-modelling of Kazakhstan low-grade coal burning in power boilers of thermal power plant with application of plasma gasification and stabilization technologies. Journal of Physics: Conference Series, 1261 (1), 012022. https://doi.org/10.1088/1742-6596/1261/1/012022
2. Mislyuk, O., Khomenko, E., Yehorova, O., Zhytska, L. (2023). Assessing risk caused by atmospheric air pollution from motor vehicles to the health of population in urbanized areas. Eastern-European Journal of Enterprise Technologies, 1 (10 (121)), 19–26. https://doi.org/10.15587/1729-4061.2023.274174
3. Zaporozhets, O., Synylo, K., Karpenko, S., Krupko, A. (2021). Improvementof the computer model of air pollution estimation due to emissions of stationary sources of airports and compressor stations. Eastern-European Journal of Enterprise Technologies, 3 (10 (111)), 54–64. https://doi.org/10.15587/1729-4061.2021.236125
4. Bolegenova, S. A. (2024). Simulation of liquid fuel spray formation and distribution in a reacting turbulent flow. Eurasian Physical Technical Journal, 21 (2 (48)), 22–30. https://doi.org/10.31489/2024no2/22-30
5. Ritchie, H., Roser, M. (2022). Our World in Data. Kazakhstan: CO_2 Country Profile. Available at: https://ourworldindata.org/co2/country/kazakhstan
6. Kazakhstan Greenhouse Gas (GHG) Emissions 1990-2024. Available at: https://www.macrotrends.net/global-metrics/countries/KAZ/kazakhstan/ghg-greenhouse-gas-emissions
7. Ecological indicators of environmental monitoring and assessment. Bureau of National Statistics of the Agency for Strategic planning and reforms of the Republic of Kazakhstan. Available at: https://stat.gov.kz/en/ecologic-indicators/28463/greenhouse_gas_emissions/
8. Statistics of environment. Key indicators. Bureau of National Statistics of the Agency for Strategic planning and reforms of the Republic of Kazakhstan. Available at: https://stat.gov.kz/en/industries/environment/stat-eco/

9. Askarova, A., Bolegenova, S., Maximov, V., Bekmukhamet, A., Gabitova, Z., Beketayeva, M. (2014). Control of Harmful Emissions Concentration into the Atmosphere of Megacities of Kazakhstan Republic. IERI Procedia, 10, 252–258. https://doi.org/10.1016/j.ieri.2014.09.085
10. Bolegenova, S., Askarova, A., Ospanova, S., Zhumagaliyeva, S., Makanova, A., Aldiyarova, A. et al. (2024). Technology of reducing greenhouse gas emissions for decarbonization and decreasing anthropogenic pressure on the environment. Physical Sciences and Technology, 11 (1-2), 64–75. https://doi.org/10.26577/phst2024v11i1a8
11. Reitz, R. D. (1987). Modeling atomization processes in high-pressure vaporizing sprays. Atomization and Spray Technology, 3, 309–337. Available at: https://uwmadison.app.box.com/v/AandS
12. Villermaux, E. (2007). Fragmentation. Annual Review of Fluid Mechanics, 39 (1), 419–446. https://doi.org/10.1146/annurev.fluid.39.050905.110214
13. Yi, Y., Reitz, R. D. (2004). Modeling the primary breakup of high-speed jets. Atomization and Sprays, 14 (1), 53–80. https://doi.org/10.1615/atomizspr.v14.i1.40
14. Tanner, F. X. (2004). Development and validation of a cascade atomization and drop breakup model for high-velocity dense sprays. Atomization and Sprays, 14 (3), 211–242. https://doi.org/10.1615/atomizspr.v14.i3.20
15. Anez, J., Ahmed, A., Hecht, N., Duret, B., Reveillon, J., Demoulin, F. X. (2019). Eulerian-Lagrangian spray atomization model coupled with interface capturing method for diesel injectors. International Journal of Multiphase Flow, 113, 325–342. https://doi.org/10.1016/j.ijmultiphaseflow.2018.10.009
16. Arcoumanis, C., Gavaises, M. (1998). Linking nozzle flow with spray characteristics in a diesel fuel injection system. Atomization and Sprays, 8 (3), 307–347. https://doi.org/10.1615/atomizspr.v8.i3.50
17. Andriotis, A., Gavaises, M., Arcoumanis, C. (2008). Vortex flow and cavitation in diesel injector nozzles. Journal of Fluid Mechanics, 610, 195–215. https://doi.org/10.1017/s0022112008002668
18. Andriotis, A., Gavaises, M. (2009). Influence of vortex flow and cavitation on near-nozzle diesel spray dispersion angle. Atomization and Sprays, 19 (3), 247–261. https://doi.org/10.1615/atomizspr.v19.i3.30
19. Berezovskaya, I. E. (2023). Investigation of the influence of liquid fuel injection rate on the combustion process using KIVA-II software. Eurasian Physical Technical Journal, 20(3(45)), 43–51. https://doi.org/10.31489/2023no3/43-51
20. Gorokhovski, M. A., Oruganti, S. K. (2021). Stochastic models for the droplet motion and evaporation in under-resolved turbulent flows at a large Reynolds number. Journal of Fluid Mechanics, 932. https://doi.org/10.1017/jfm.2021.916
21. Han, Z., Fan, L., Reitz, R. D. (1997). Multidimensional Modeling of Spray Atomization and Air-Fuel Mixing in a Direct-Injection Spark-Ignition Engine. SAE Technical Paper Series. https://doi.org/10.4271/970884
22. Khan, M. M., Hélie, J., Gorokhovski, M. (2018). Computational methodology for non-evaporating spray in quiescent chamber using Large Eddy Simulation. International Journal of Multiphase Flow, 102, 102–118. https://doi.org/10.1016/j.ijmultiphaseflow.2018.01.025
23. Dhande, D. Y., Sinaga, N., Dahe, K. B. (2021). Study on combustion, performance and exhaust emissions of bioethanol-gasoline blended spark ignition engine. Heliyon, 7 (3), e06380. https://doi.org/10.1016/j.heliyon.2021.e06380
24. Sahoo, S., Srivastava, D. K. (2023). Numerical analysis of performance, combustion, and emission characteristics of PFI gasoline, PFI CNG, and DI CNG engine. Energy, 278, 127749. https://doi.org/10.1016/j.energy.2023.127749
25. Askarova, A., Bolegenova, S., Ospanova, Sh., Slavinskaya, N., Aldiyarova, A., Ungarova, N. (2021). Simulation of non-isothermal liquid sprays under large-scale turbulence. Physical Sciences and Technology, 8 (2). https://doi.org/10.26577/phst.2021.v8.i2.04
26. Chang, M., Kim, H., Zhou, B., Park, S. (2023). Spray collapse resistance of GDI injectors with different hole structures under flash boiling conditions. Energy, 268, 126689. https://doi.org/10.1016/j.energy.2023.126689
27. Oruganti, S. K., Gorokhovski, M. A. (2024). Stochastic models in the under-resolved simulations of spray formation during high-speed liquid injection. Physics of Fluids, 36 (5). https://doi.org/10.1063/5.0206826
28. Askarova, A., Bekmukhamet, A., Bolegenova, S., Ospanova, S., Symbat, B., Maximov, V. et al. (2016). 3-D Modeling of Heat and Mass Transfer during Combustion of Solid Fuel in Bkz-420-140-7C Combustion Chamber of Kazkhstan. Journal of Applied Fluid Mechanics, 9 (2), 699–709. https://doi.org/10.18869/acadpub.jafm.68.225.22881
29. Leithner, R., Askarova, A., Bolegenova, S., Bolegenova, S., Maximov, V., Ospanova, S. et al. (2016). Computational modeling of heat and mass transfer processes in combustion chamber at power plant of Kazakhstan. MATEC Web of Conferences, 76, 06001. https://doi.org/10.1051/matecconf/20167606001
30. Bolegenova, S., Askarova, A., Slavinskaya, N., Ospanova, Sh., Maxutkhanova, A., Aldiyarova, A., Yerbosynov, D. (2022). Statistical modeling of spray formation, combustion, and evaporation of liquid fuel droplets. Physical Sciences and Technology, 9 (2). https://doi.org/10.26577/phst.2022.v9.i2.09
31. Khan, M. M., Hélie, J., Gorokhovski, M., Sheikh, N. A. (2017). Experimental and numerical study of flash boiling in gasoline direct injection sprays. Applied Thermal Engineering, 123, 377–389. https://doi.org/10.1016/j.applthermaleng.2017.05.102
32. Gorokhovski, M., Jouanguy, J., Chtab-Desportes, A. (2009). Stochastic model of the near-to-injector spray formation assisted by a high-speed coaxial gas jet. Fluid Dynamics Research, 41 (3), 035509. https://doi.org/10.1088/0169-5983/41/3/035509

33. Arcoumanis, C., Cutter, P., Whitelaw, D. S. (1998). Heat Transfer Processes in Diesel Engines. Chemical Engineering Research and Design, 76 (2), 124–132. https://doi.org/10.1205/026387698524695
34. Huang, J., Zhao, X. (2019). Numerical simulations of atomization and evaporation in liquid jet flows. International Journal of Multiphase Flow, 119, 180–193. https://doi.org/10.1016/j.ijmultiphaseflow.2019.07.018
35. García-Contreras, R., Armas, O., Mata, C., Villanueva, O. (2017). Impact of Gas To Liquid and diesel fuels on the engine cold start. Fuel, 203, 298–307. https://doi.org/10.1016/j.fuel.2017.04.116
36. Dhar, A., Tauzia, X., Maiboom, A. (2016). Phenomenological models for prediction of spray penetration and mixture properties for different injection profiles. Fuel, 171, 136–142. https://doi.org/10.1016/j.fuel.2015.12.022
37. Zhu, L., Wu, K., Zhang, E., She, Y., Zhan, W., Liu, Q. (2015). A modified model for calculating Theoretical Flame Temperature in blast furnace and its application. Journal of Iron and Steel Research International, 22 (1), 9–14. https://doi.org/10.1016/s1006-706x(15)60002-4